Strain-Dependent Damping of Ti–10V–2Fe–3Al at Room Temperature

J. Göken[a,*], S. Fayed[a] and P. Skubisz[b]

[a]University of Applied Sciences Emden-Leer, Faculty of Maritime Studies, Bergmannstr. 36, 26789 Leer, Germany

[b]Faculty of Metals Engineering and Industrial Computer Science, AGH University of Science and Technology, al. A. Mickiewicza 30, 30-059 Krakow, Poland

(Received April 25, 2016; in final form October 20, 2016)

The Ti–10V–2Fe–3Al alloy is advantageous over other titanium grades due to its high tensile strength and its high resistance against creep, cracking, and corrosion. The investigated alloy was hammer-forged inducing high strain rates in the material at a temperature of 800 °C and underwent different cooling procedures. Three in that way thermomechanically treated specimens were prepared for subsequent study of the vibration behaviour of the material with the help of non-destructive, contact-free acoustic measurements. Resulting time-dependent decaying acoustic signals were analysed to investigate the dependence of the material damping behaviour on the individual downstream thermal treatment procedure and, ultimately, on the microstructural changes.

DOI: 10.12693/APhysPolA.130.1352

PACS/topics: 61.72.Hh, 43.40.Cw, 43.58.Fm

1. Introduction

Lightweight designs offer a major contribution regarding reduced fuel consumption in several transportation fields and, thus, reduced CO_2 emissions. An effective way to minimise the weight without major changes in the design is the substitution of construction materials with high specific density, such as steels, by lighter titanium alloys [1, 2] with simultaneous maintaining of the strength.

Especially in the marine industry, titanium is a suitable construction material due to its low density (roughly half the weight of steel, nickel and copper alloys), its high strength-to density ratio, its high temperature resistance (up to 600 °C), and its remarkable corrosion/erosion resistance [3].

Moreover, titanium alloys offer a manufacturing versatility due to their availability in different structural states presenting different allotropic microstructural changes, such as α- and β-titanium alloys [4]. Therefore, recent research studies on titanium alloys are concerned with the investigations of different thermo-mechanical processing methods and their influence on the mechanical behaviour of titanium alloys, involving elastic/plastic deformations, fatigue, creep, fracture [5], and damping [6].

2. Experimental

The material used for the applied experiments in this work was the near β-alloy Ti–10V–2Fe–3Al which is also known as Ti–10–2–3. Its chemical composition is shown in Table I.

TABLE I

Chemical composition [wt%] of the Ti–10V–2Fe–3Al alloy.

C	V	Al	Fe	N	O	H	Y	Ti
0.024	9.76	3.37	1.84	0.016	0.10	0.0001	< 0.005	balance

Al is one of the most important α-phase stabilising elements. The interstitials O, N, and C tend to stabilise the α-phase, too, whereas V and Fe are regarded as β-phase stabilising elements because of lowering the temperature of transformation (from α-titanium alloy to β-titanium alloy) [7, 8].

2.1. Processing conditions

The investigated alloy was thermomechanically processed in a sequence of hot forging and varied conditions of solution treatment and subsequent ageing. The variation in cooling manner aimed at producing obvious difference in the final microstructure.

Forging was realised in industrial conditions with a drop-forging hammer using a blow energy of 16 kJ. Two samples with initial height of 20 mm were flattened in 4-hit cogging operation to a final height of 2 mm. A natural strain value of 2.3 was achieved which corresponded to the numerically estimated effective strain value of 2.5. Other than low-strain-forging which is commonly applied to activate the recrystallisation process (grain refinement) [9], the applied forging method suggested high strain rate deformation as an alternative for isothermal or cost-intensive hot die forging.

A considerable fact about a thermo-mechanical treatment is the β-transus temperature (β-transus temperature of Ti–10–2–3 is 795 °C [10]), since it separates the single β-phase field from the two-phase ($\alpha + \beta$)-field [4]. The specimens were heated up to 800 °C. This means

*corresponding author; e-mail: juergen.goeken@hs-emden-leer.de

that the deformation started over that β-transus point. In incremental-like manner of forging, the temperature of the section being forged increased by approximately 40 degrees, while the rest was cooling down. With passing to the next section, the process was repeated in that particular section, while the remaining portion was naturally chilled. The end temperature of the forged samples dropped below the transus point, finally reaching 770 °C.

After deformation, the specimens were slowly cooled down in air and then quenched in water. Owing to fast cooling, no transformation occurred and the microstructure still consisted of β-phase grains at this final temperature which is evident from the micrograph in Fig. 1, where only the surface layer is transformed (the layer was machined, and had no effect on mechanical behaviour). The processing cycles formed a microstructure consisting of refined β grains and α particles of varied morphology, dispersion and size. The saturated state allowed subsequent ageing.

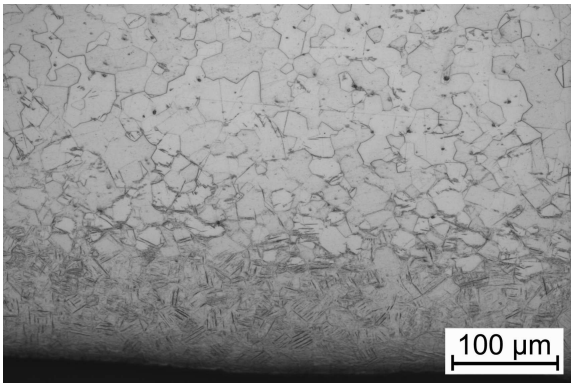

Fig. 1. Microstructure of the Ti–10–2–3 sample after forging process.

Since the cooling procedure has an important influence on the microstructural development of the investigated Ti-alloy, three Ti–10–2–3 specimens were processed as follows: the first sample was hammer-forged and cooled in air, the second one was hammer-forged and quenched in water and the third one was hammer-forged, quenched in water and aged (520 °C for 2 h).

The specimens were cut out for metallographic work and acoustic measurements which were carried out on bending beams of 120 mm length (bending length: about 88 mm), 10 mm width and 2 mm thickness.

2.2. Acoustic system

2.2.1. Experimental setup

The structure-sensitive material damping was determined by acoustic measurements. A sketch of the used experimental setup is shown in Fig. 2. It consisted of a crank which was attached to a roller on which a tooth was mounted. After rotating the roller manually, the tooth touched the free end of the bending beam and pressed the beam down to a predetermined deflection. Subsequently, the sample performed a freely decaying oscillation (i.e. vibration at the natural resonant frequency) after the tooth had passed the free end of the bending beam.

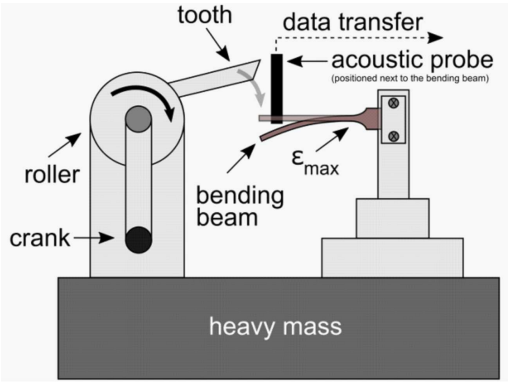

Fig. 2. Experimental setup of the applied acoustic measurements [11].

An acoustic probe (Microflown™ probe, Microflown Technologies, NL) was positioned perpendicularly, near the clamped side of the sample with a distance of about 30 mm from it. The impact of parasitic effects like air vortexes could be reduced by choosing this positioning distance of the probe from the sample. This special sensor consists of very sensitive pressure and particle velocity microphones. Its acoustical properties are shown in Table II.

TABLE II

Acoustical properties of the Microflown™ probe [12].

	Frequency range	Upper sound level	Polar pattern	Directivity
sound pressure sensor	20 Hz–10 kHz	110 dB	omnidirectional	omnidirectional
particle velocity sensor	0.1 Hz–10 kHz	125 dB	figure of eight	directive

First own measurements to determine the material damping by means of the used sensitive acoustic sensor from the freely decaying flexural vibration of a bending beam were published in Ref. [13].

2.2.2. Acoustic measurements

The temporal decay of the acoustic measurements is dependent on the material damping, which is physically based on the transformation of mechanical energy into heat. Thus, as a first step, time-dependent vibration measurements were applied in this study to get an impression of the influence of thermo-mechanical treatment on the vibration behaviour of the three differently processed Ti–10–2–3 specimens. The resonance frequency of each sample, obtained from the acoustic data,

was measured and compared to the corresponding fundamental frequency value which was calculated on the basis of technical mechanics of vibrating beams. The calculated values were in good agreement with the measured ones using the probe (≈185 Hz).

After the mechanical excitation of the bending beam, the time-dependent sound pressure data values were digitally recorded by a two-channel signal conditioner at a sampling rate of 5 kHz and then transferred to the computer. 25 successive measurements at 5 different flexural vibration amplitudes (different sample deflections) were performed on each Ti–10–2–3 sample. These measurements served on the one hand for the investigation of the relationship between the bending deflections of the samples and the resulting sound pressure values, and on the other hand, for studying the damping behaviour of different Ti–10–2–3 samples as a function of the strain.

Figure 3 shows the steps of the data processing applied on the raw data (inserted figure) of the time-resolved sound pressure signal coming out of the signal conditioner. The background signal accompanying each of the vibration measurements was recorded and eliminated from the total output signal in order to obtain a relatively denoised sound pressure signal of the excited sample.

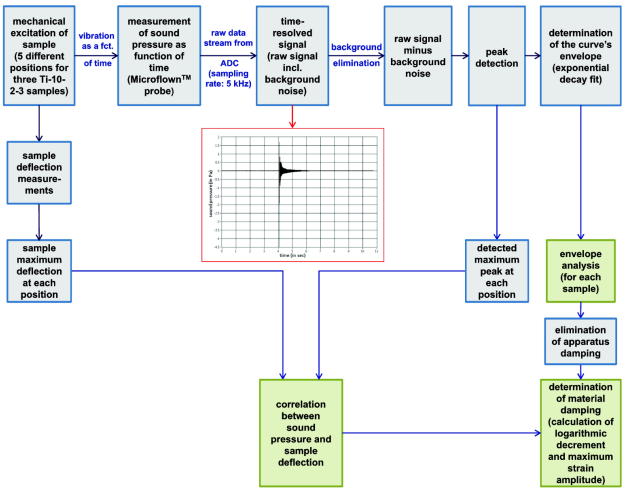

Fig. 3. Data processing steps (blue: raw data treatment, green: data processing results), inserted plot: raw data of the measured sound pressure [Pa] versus the time [s] of the Ti–10–2–3 sample being as-forged and cooled in air.

The effect of the experimental setup's vibration, which occurs when the vibration energy of the sample is transferred to whole setup (e.g. through the sample holder), could be experimentally reduced using energy absorbing materials in those locations where the transfer of vibration energy was distinctly high. Although the apparent part of the setup damping was diminished, a still existing residual effect of the apparatus damping had to be approximately estimated and eliminated during the data processing, too, since apparatus damping can be superimposed on the material damping. This kind of damping was determined using a stiff reference sample (NiCr19NbMo, a high-strength, corrosion-resistant nickel chromium material) of 122 mm length (bending length: about 90 mm), 8 mm width and 2 mm thickness (resonance frequency ≈247 Hz). As a result of its very low damping capacity, other effects (e.g. damping by external friction due to clamping) became more dominant and could be identified as a residual apparatus damping. This value was subtracted from the measured damping of the Ti–10–2–3 samples (see Fig. 3).

2.2.3. Relationship between sound pressure amplitude and sample deflection

It was assumed that the maximum measured sound pressure values S_n $(n = 0, 1, 2, ...)$ received by the Microflown™ probe can be directly assigned to the current mechanical deflection z'_n. From the above mentioned 25 applied measurements, the mean values and their individual standard deviation of the resulting flexural vibration amplitudes z'_n for a chosen sound pressure value S_n were taken into account. In Fig. 4, the deflection z'_n is plotted versus the sound pressure signal S_n.

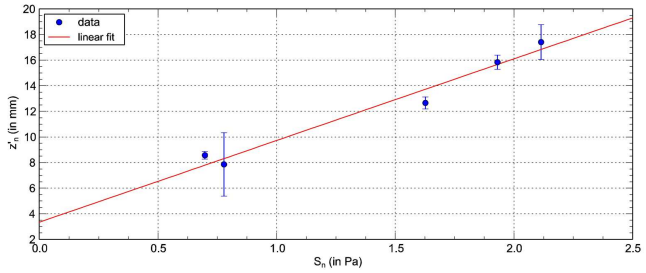

Fig. 4. Correlation between the maximum values of the sound pressure amplitudes S_n and the corresponding sample deflection z'_n.

The curve was linearly fitted and the slope of the curve was calculated using Eq. (1),

$$c = \frac{\Delta z'_n}{\Delta S_n}. \tag{1}$$

These acoustic measurements verified that the maxima of the decaying sound pressure can, in a good approximation, directly be attributed to the corresponding temporal decrease of the sample deflections (amplitudes of flexural vibration).

3. Results and discussion

The micrographs representing the microstructural changes after the above-described processing variants are shown in Fig. 5a–c. The as-forged water-cooled material represents typical solution treated condition of the alloy with recrystallised grain and scarce precipitates (Fig. 5a). The air-cooled material exhibited more precipitates (Fig. 5b). In fact, the alloy was abundant in a variety of particles, which indicates that the low cooling rate was ineffective to saturate the alloy. The air-cooled

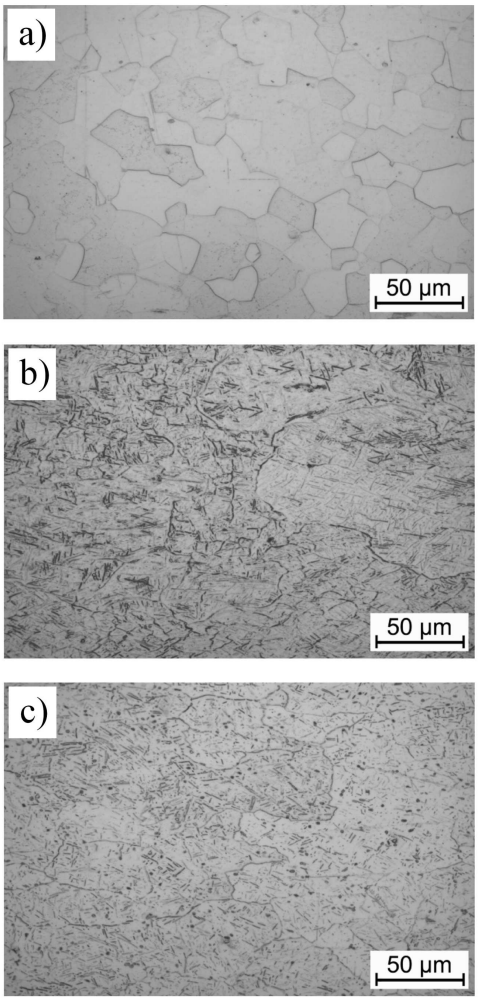

Fig. 5. Microstructure of the Ti–10–2–3 sample: (a) hammer-forged and cooled in air, (b) hammer-forged and quenched in water, (c) hammer-forged, quenched in water and aged (520 °C for 2 h).

microstructure was qualitatively similar to that after ageing (Fig. 5c). However, the differences in aspect ratio of the obtained α precipitates produced on cooling and those obtained through ageing, which is of the critical meaning as for the strength-ductility property relations in Ti β-alloys, are strong enough to be detected by acoustic response on the material.

In order to analyse if there is a variation in the decay behaviour of the acoustic output signal, indicating microstructural differences, the reduction of the sound pressure amplitude as a function of time t was recorded as a first step. The maxima (peak values) of the time-dependent acoustic signal were determined with the help of a self-written program in LabVIEW from National Instruments™ using a parabolic curve fit. An exponential decay fit (Eq. (2)) of the obtained peak values $S(t)$ was then applied on the decaying output signal. The peak values can be written as

$$S(t) = S_0\,\mathrm{e}^{-\beta t} + b, \tag{2}$$

where S_0 is the initial sound pressure amplitude, $S(t)$ is the time-dependent sound pressure amplitude and b is a constant offset. Since the actual measurement started after some seconds of the recording, only data points starting from the maximum vibration amplitude and afterwards were taken into account. This means that signal turbulences occurring at the beginning of each measurement due to preponderant vibration of the equipment had been ignored.

The damping constant β could be determined from the decay of the signal's envelope curves, shown in Fig. 6 for the three investigated Ti–10–2–3 samples.

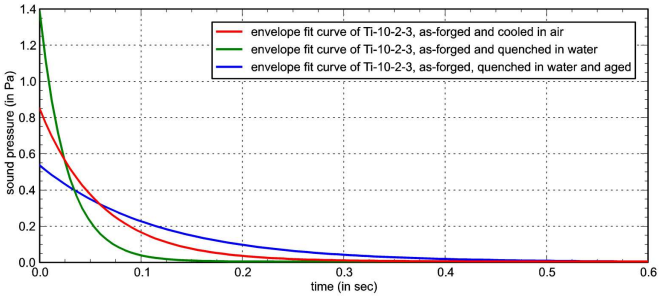

Fig. 6. Envelope fit curves of the detected peak values.

The corresponding damping constants β from Eq. (2) for the three Ti–10–2–3 samples are listed in Table III.

TABLE III

Damping constants.

Condition	As-forged and cooled in air	As-forged and quenched in water	As-forged, quenched in water and aged
β [s^{-1}]	16.6	36.8	8.6

The varying values emphasise that the specimens have different microstructures and this should lead to significant changes in strain-dependent damping measurements. The maximum strain $\varepsilon_{\max}$ in the material is dependent on the current amplitude of the flexural vibration [14] and can be calculated as follows:

$$\varepsilon_{\max} = \frac{3a}{2l^2} z', \tag{3}$$

where a and l represent the thickness and the length of the sample, respectively, and z' is the amplitude of the flexural vibration (deflection) of the sample. Using Eq. (3) and Eq. (1), the current maximum strain values $\varepsilon_{\max,n}$ can be determined from the current sound pressure amplitude $S_\mathrm{n}(t)$ as

$$\varepsilon_{\max,n} = \frac{3a}{2l^2} c S_\mathrm{n}(t). \tag{4}$$

The logarithmic decrement method had been used to determine the damping of the investigated samples in time domain. It is assumed that the temporal decay of the sound pressure amplitudes corresponds to the temporal decay of the amplitudes of the flexural vibration. Thus, the material damping could be received by measurements of $S_\mathrm{n}(t)$. Taking the drop of the sound pressure amplitude in k successive cycles into consideration, the logarithmic decrement δ is obtained from

$$\delta = \frac{1}{k}\ln\left(\frac{S_{\mathrm{n}}(t)}{S_{\mathrm{n+k}}(t)}\right), \tag{5}$$

where $S_{\mathrm{n}}(t)$ is the sound pressure amplitude at the time nT (T: cycle time) and $S_{\mathrm{n+k}}(t)$ is the drop of amplitude in k successive cycles later at the time $(n+k)T$ in free decay vibration [15].

It was found that the apparatus damping δ_a taken from δ-values at very low $\varepsilon_{\max}$ is strongly dependent on individual acoustical conditions being changeable e.g. by slightly different positioning of the probe after sample changing. Therefore, not only the data of the reference sample but also those of the titanium specimens were used to calculate an average apparatus damping $\overline{\delta_a}$. $\overline{\delta_a} \approx 12 \times 10^{-3}$ could be assessed. This value was subtracted from the calculated logarithmic decrement δ of the used Ti–10–2–3 samples (see Fig. 3). Taking the well-established low damping behaviour of titanium into account, the resulting fitted strain-dependent damping curves for the titanium samples showed unexpected high δ-values (Fig. 7, inserted diagram). This could be explained as follows. During the sound propagation in air, the acoustic energy is always reduced by friction, conduction of heat, and excitation of intramolecular vibrations [16]. This means that, in addition to the energy dissipation in the solid, energy dissipation in air can be expected, which leads to a higher material damping than estimated.

At a maximum strain amplitude $\varepsilon_{\max} = 1 \times 10^{-3}$, the reference sample showed a δ-value that was 100 times higher than an obtained value in earlier own studies. Therefore, an approximation of the resulting data had been applied by dividing the experimentally obtained data by the value 100, Fig. 7.

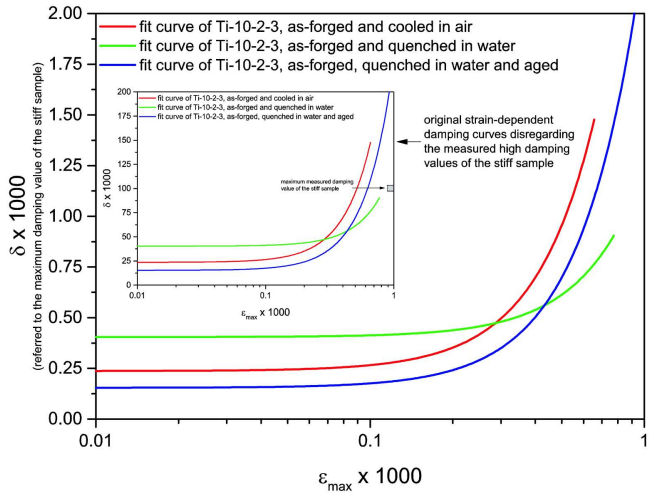

Fig. 7. Fitted strain-dependent damping curves of Ti–10–2–3 samples after different thermal treatment procedures.

A various strain dependence of the damping behaviour of the differently thermally heat treated hammer-forged samples could be observed. All curves showed a strain-independent (δ_0) and a strain-dependent part (δ_h). It is obvious that the sample which was hammer-forged and quenched in water tended to have the highest damping value (this value can be mainly referred to δ_0), as approximately expected from the damping constants β (see Table III) or envelope fit curves (see Fig. 6). The corresponding microstructure (Fig. 5b) was characterised by a high amount of precipitates. This means a flagrant impoverishment of atoms in the matrix which has a significant impact on the material damping [17].

It can be assumed that dislocation damping is the main source of the experimentally received curve progression. The damping mechanism is explained by the Koehler–Granato–Lücke (K–G–L) vibrating string model proposed by Koehler [18] and developed further by Granato and Lücke [19], Fig. 8. Experimental findings of Bleasdale and Bacon [20] approved this assumption and proposed that high strains increase the mobile dislocation density and thus increase the damping at lower strains.

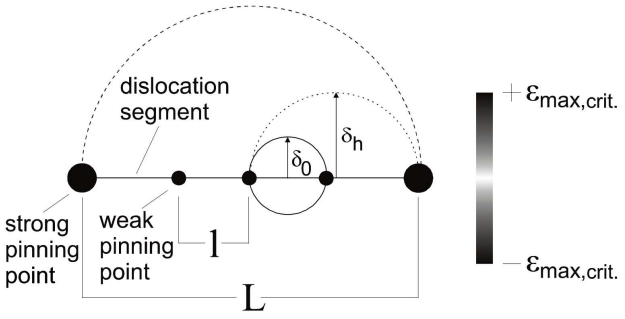

Fig. 8. Pinning and bowing out of a dislocation segment according to the K–G–L model. l — dislocation segment between weak pinning points, L — dislocation segment between strong pinning points.

The value of the strain-independent logarithmic decrement δ_0 is proportional to the product of the dislocation density Λ and the fourth power of the average distance between weak pinning points on dislocations, i.e. $\delta_0 \propto \Lambda l^4$ [21, 22]. In case of precipitation development, the distance between the strong pinning points of the matrix becomes larger. As a consequence, the dislocation segment is more moveable which leads to a higher damping. It could be observed that subsequent ageing after water quenching resulted in a distinct reduction of damping. This can be attributed to a re-pinning of the dislocations because some precipitations were dissolved again.

Moreover, a higher maximum strain amplitude for a break-away of dislocations from pinning points for the water-cooled sample was detected. This gives an indication that the dislocations are less movable due to the rapid cooling which can be traced to higher stresses in the material.

4. Conclusions

The Ti–10V–2Fe–3Al alloy (Ti–10–2–3), which is characterised by its high tensile strength and high resistance

against creep, underwent a high strain rate deformation as an alternative for isothermal or cost-intensive hot die forging. Since the cooling process has a strong influence on the microstructural development, especially by the evolution of precipitates, structure-sensitive damping measurements were carried out on different Ti–10–2–3 samples (hammer-forged and cooled in air; hammer-forged and quenched in water; hammer-forged, quenched in water and aged (520 °C for 2 h)) using an acoustic setup.

It was found that the decaying sound pressure can, in a good approximation, directly be attributed to the corresponding temporal decrease of the sample deflections. Based on this correlation, the logarithmic decrement method has been used to measure the material damping as a function of the maximum strain amplitude of the sample. The obtained results were in correlation with the sequence of the material damping of Ti–10–2–3 samples as received from the slope of the decay curves of sound pressure measurements.

The curve progression of the strain-dependent damping curves was explained in the framework of the K–G–L string model where dislocations are pinned by strong and weak pinning points. When precipitation takes place, the matrix becomes depleted in atoms which leads to a stronger bowing out of dislocation segments and, thus, to a higher material damping. This could be observed for the Ti–10–2–3 sample which was hammer-forged and quenched in water whereas the amount of precipitations was expected to be reduced by ageing because the material damping was lower. The strain dependence of the damping of the Ti-specimen which was hammer-forged and cooled in air allows the conclusion that the dislocations are pinned more strongly which can be due to high stresses in the material by this cooling procedure.

Acknowledgments

Professor Dr. Jürgen Göken gratefully acknowledges the financial support of the German Research Foundation (DFG, www.dfg.de; DFG-reference number: INST 21572/1-1 LAGG).

References

[1] G. Srinivasu, Y. Natraj, A. Bhattacharjee, T.K. Nandy, G.V.S. Nageswara Rao, *Mater. Des.* **47**, 323 (2013).

[2] M. Jackson, N.G. Jones, D. Dye, R.J. Dashwood, *Mater. Sci. Eng. A* **501**, 248 (2009).

[3] RMI Titanium Company, *Titanium Alloy Guide*, RTI International Metals, January 2000. Available: www.rtiintl.com (accessed 1 September 2015).

[4] M. Peters, J. Hemptenmacher, J. Kumpfert, C. Leyens, in: *Titanium and Titanium Alloys — Fundamentals and Applications*, Eds. C. Leyens, M. Peters, Wiley-VCH, Weinheim 2003, p. 1.

[5] P. Skubisz, M. Packo, K. Mordalska, T. Skowronek, *Adv. Mater. Res.* **845**, 96 (2014).

[6] Y.K. Favstov, Y.A. Samoilov, *Met. Sci. Heat Treat.* **25**, 679 (1983).

[7] I. Weiss, S.L. Semiatin, *Mater. Sci. Eng. A* **243**, 46 (1998).

[8] S. Ankem, C.A. Greene, *Mater. Sci. Eng. A* **263**, 127 (1999).

[9] S. Bruschi, S. Poggio, F. Quadrini, M.E. Tata, *Mater. Lett.* **58**, 3622 (2004).

[10] *Titanium, Physical Metallurgy, Processing, and Applications*, Ed. F.H. Froes, ASM International, Materials Park, Ohio, USA 2015.

[11] J. Göken, S. Fayed, P. Skubisz, in: *Proc. Int. Conf. on Lightweight Design of Marine Structures (LIMAS 2015)*, ASRANet Ltd, Glasgow (Scotland) 2015, p. 156.

[12] www.microflown.com, retrieval dated 3 September 2015, "Microflown™ Technologies, Charting sound fields, Manual PU — regular, MFPA-V1.0 2014".

[13] J. Göken, J. Swiostek, H. Hurdelbrink, U. Keil, *Acta Metall. Sin. (Engl. Lett.)* **26**, 113 (2013).

[14] I.S. Golovin, H.-R. Sinning, J. Göken, W. Riehemann, *Solid State Phenom.* **89**, 267 (2003).

[15] W. Riehemann, *Metallic Materials with Extreme Internal Friction and their Measurement*, Papierflieger Verlag, Clausthal-Zellerfeld 1996 (in German).

[16] F. Trendelenburg, *Introduction into Acoustics*, Springer, Berlin 1939 (in German).

[17] J. Göken, W. Riehemann, *Mater. Sci. Eng. A* **324**, 127 (2002).

[18] J.S. Koehler, in: *Imperfections in Nearly Perfect Crystals*, Eds. W. Shockley, J.H. Hollomon, R. Maurer, F. Seitz, Wiley, New York 1952, p. 197.

[19] A.V. Granato, K. Lücke, *J. Appl. Phys.* **27**, 583 (1956).

[20] P.A. Bleasdale, D.J. Bacon, in: *Internal Friction and Ultrasonic Attenuation in Solids: Proceedings of the Third European Conf.*, Ed. C.C. Smith, Pergamon Press, Oxford 1980, p. 173.

[21] Z. Trojanová, P. Lukáč, W. Riehemann, B.L. Mordike, *Mater. Sci. Eng. A* **226-228**, 867 (1997).

[22] A.S. Nowick, B.S. Berry, *Anelastic Relaxation in Crystalline Solids*, Academic Press, New York 1972.